RESEARCH ARTICLE

Key Points:
- The feasibility of a nationwide EEWS in Italy is for the first time assessed
- The analysis is extended also to regions that did not experience earthquakes
- Higher seismic hazard areas could benefit from lead times of about 25 s

Correspondence to:
M. Picozzi,
matteo.picozzi@unina.it

Exploring the feasibility of a nationwide earthquake early warning system in Italy

M. Picozzi[1], A. Zollo[1], P. Brondi[1], S. Colombelli[1,2], L. Elia[1,2], and C. Martino[1,2]

[1]Department of Physics, Università degli Studi di Napoli Federico II, Naples, Italy, [2]RISSC Laboratory, AMRA Scarl, Naples, Italy

Abstract When accompanied by appropriate training and preparedness of a population, Earthquake Early Warning Systems (EEWS) are effective and viable tools for the real-time reduction of societal exposure to seismic events in metropolitan areas. The Italian Accelerometric Network, RAN, which consists of about 500 stations installed over all the active seismic zones, as well as many cities and strategic infrastructures in Italy, has the potential to serve as a nationwide early warning system. In this work, we present a feasibility study for a nationwide EEWS in Italy obtained by the integration of the RAN and the software platform PRobabilistic and Evolutionary early warning SysTem (PRESTo). The performance of the RAN-PRESTo EEWS is first assessed by testing it on real strong motion recordings of 40 of the largest earthquakes that have occurred during the last 10 years in Italy. Furthermore, we extend the analysis to regions that did not experience earthquakes by considering a nationwide grid of synthetic sources capable of generating Gutenberg-Richter sequences corresponding to the one adopted by the seismic hazard map of the Italian territory. Our results indicate that the RAN-PRESTo EEWS could theoretically provide for higher seismic hazard areas reliable alert messages within about 5 to 10 s and maximum lead times of about 25 s. In case of large events ($M > 6.5$), this amount of lead time would be sufficient for taking basic protective measures (e.g., duck and cover, move away from windows or equipment) in tens to hundreds of municipalities affected by large ground shaking.

1. Introduction

The dramatic increase of vulnerability to earthquakes of metropolitan areas over the last decade and the very low probability level at which short-term earthquake forecasting is still feasible has led to Earthquake Early Warning Systems (EEWS) to be considered as a very effective and viable contribution to the real-time reduction of societal exposure to seismic risk in cities [*Gasparini et al.*, 2010]. Over the last few decades, the theoretical and methodological advances in real-time data analysis have been accompanied by a rapid improvement in telemetry and computer technology. Hence, nowadays, a number of EEWS are already operating worldwide or are being developed (e.g., Japan, Taiwan, Mexico, Italy, Turkey, California, Israel, etc., among others) [*Allen et al.*, 2009; *Allen and Kanamori*, 2003; *Kanamori*, 2005; *Pinsky*, 2014].

Typically, *P* wave based EEWS follow two basic approaches: "*regional*" (or *network based*) and "*on-site*" warning. The key parameter for any early warning system is the "*lead time*," which is the time available for protective measures to be taken at distant targets once an earthquake has been promptly detected and characterized, and an alarm issued. From the practical point of view, the lead time changes according to the EEWS typology. Regional EEWS are based on the use of a seismic network located near the expected epicentral areas. Their aim is to detect and locate an earthquake and to determine its magnitude from the analysis of the first few seconds of the arriving *P* waves at one or more stations [*Satriano et al.*, 2010]. The lead time for regional EEWS is defined as the travel time difference between the arrival of the first *S* waves at the target site and the early *P* wave recorded at the source area, after accounting for the necessary computation and data transmission times.

On-site EEWS, by contrast, are designed to cope with the condition of target sites being located within a seismogenic area, so that the regional EW results in a lead time too small for issuing an effective earthquake warning. *P* wave based on-site EEWS rely on seismic sensors deployed at the target site and exploit only the information carried by the fast, early *P* waves to predict the larger shaking related to the incoming *S* and surface waves (i.e., the lead time is equal to *S* minus *P* arrival times). With respect to the regional EEWS, the on-site systems are characterized by a faster warning time for targets located at near-source distance [see *Satriano et al.*, 2010, Figure 2]. However, on-site EEWS do not include robust algorithms for real-time event location, which lead them to sometimes misrecognize *P* and *S* wave arrivals and be prone to high rates of false detections. An exhaustive review of the concepts, methods, and physical basis of EEWS has been presented by *Satriano et al.* [2010].
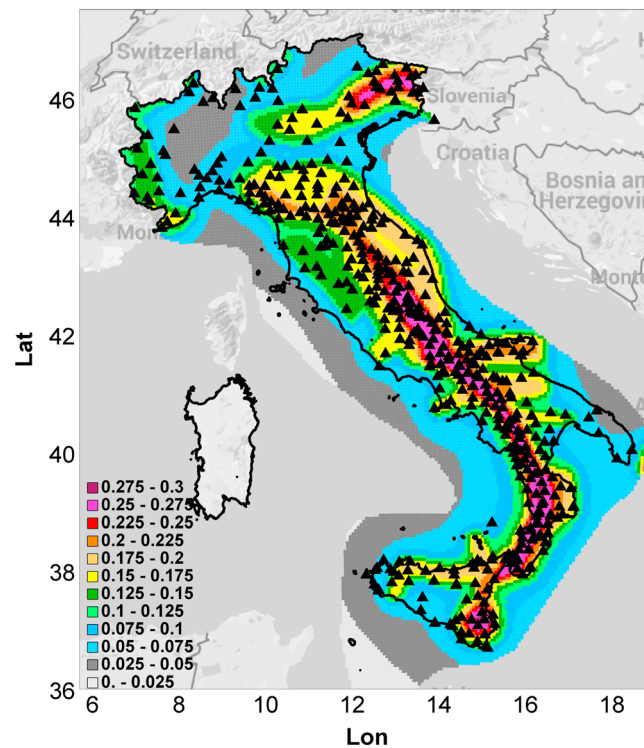
Figure 1. Seismic hazard map for Italy showing the peak ground acceleration values that have a 10% chance of being exceeded in 50 years (http://esse1-gis.mi.ingv.it/s1_en.php, redrawn), and the RAN—Italian Accelerometric Network (black triangles).

The various concepts and methodologies developed in the field of EW have led to the development of different algorithms, which are currently being tested and validated in several seismological centers around the world (e.g., among others, *Elarms* by *Allen* [2007] and Virtual Seismologist by *Cua and Heaton* [2007]). In Italy, the Seismological Laboratory at the Department of Physics, University of Naples Federico II (RISSC Lab) has developed an EW software platform named PRESTo (PRobabilistic and Evolutionary early warning SysTem) [*Iannaccone et al.*, 2009; *Satriano et al.*, 2011] for real-time data processing and seismic alert notification (http://www.prestoews.org/). In order to analyze its performance within different seismic hazard contexts and seismic networks of varying geometries, PRESTo is currently running at several seismological centers, e.g., at the Irpinia Seismic Network (ISNet) control center in Naples; at the Korean Institute of Geoscience and Mineral Resources, in South Korea; at the Kandilli Observatory and Earthquake Research Institute, in Turkey; at the National Institute of Research and Development for Earth Physics, in Romania; and at the Istituto Nazionale di Oceanografia e di Geofisica Sperimentale, in Italy.

Among the EEWS operating worldwide, the experience of the operational system implemented by the Japan Meteorological Agency (JMA) has shown the effectiveness of a combined on-site and network-based approach to rapidly broadcast warnings after a potentially damaging earthquake. As reported by *Doi* [2011], the JMA has issued EW messages to advanced users for more than 2100 earthquakes and to the public for 11 earthquakes by the end of 2009. The Japanese EEWS makes use of real-time data streamed by the extremely dense accelerometer array (more than 200 seismic stations operated by JMA and nearly 800 stations run by the National Research Institute of Earth Science and Disaster Prevention) deployed across the country [*Kamigaichi et al.*, 2009; *Doi*, 2011]. Italy has the potential for a nationwide early warning system, with more than 750 accelerometric stations installed across the whole country's active seismic zones, as well as many target cities and strategic infrastructures. However, the communications network and data streaming must be expanded and improved upon. A significant number of these stations (about 500) are nodes of the RAN (Italian Accelerometric Network) (http://www.protezionecivile.gov.it/jcms/it/ran.wp, January 2015) managed by the Italian Department of Civil Protection (DPC), whose data are used for emergency response services [*Gorini et al.*, 2010], as well as being shared with the seismological and engineering communities for technical and scientific applications.

This work aims at exploring the scientific feasibility of a nationwide EEWS in Italy that exploits the RAN and the PRESTo software system and to provide the Italian Department of Civil Protection with the necessary information for planning the implementation of an operational EEWS in Italy.

Requirements for an EEWS network include advanced, high-density, wide dynamic range data acquisition and data transmission technologies. Considering the latter, at the current stage of the development of the network, the RAN still needs an upgrade in its hardware for real-time data telemetry. Therefore, this feasibility study was carried out from a more scientific perspective, taking into account only the geometrical characteristics of the RAN, under the assumption that the hardware and the management software of the RAN will allow for real-time
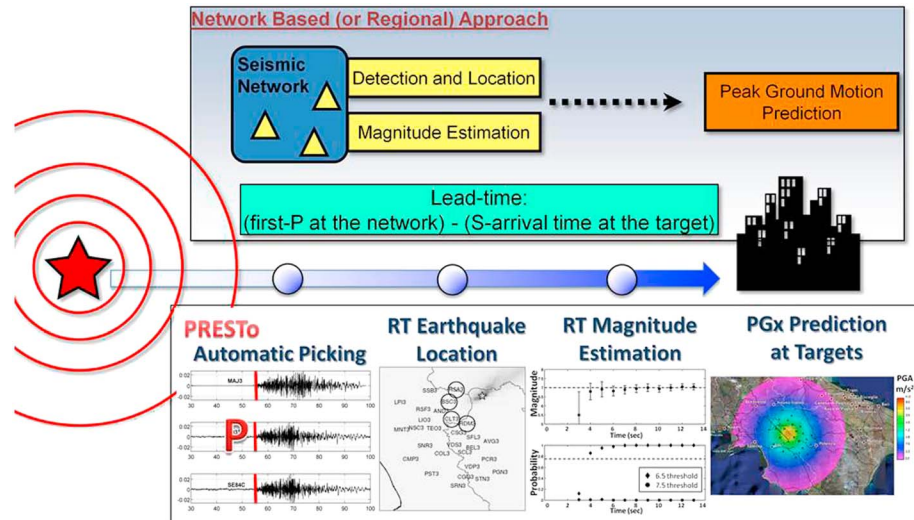
Figure 2. Schematic representation of the Regional approach for EW (modified from *Satriano et al.* [2011]), and an overview of the analyses carried out by the PRESTo software system for the real-time event characterization and prediction of the level of ground motion at target sites.

data streaming to the DPC center. Therefore, no further considerations of the necessary technical aspects related to the hardware and software requirements for real-time data telemetry within the RAN will be made.

In the following, we first summarize the main characteristics of the RAN and the principal concepts behind PRESTo. The potential of an EEWS at the national scale is evaluated by testing it on real data from 40 of the largest earthquakes that have occurred during the last 10 years in Italy and have been recorded by the RAN (made freely available by the ITalian ACcelerometric Archive, ITACA 2.0, http://itaca.mi.ingv.it/ItacaNet;) [*Luzi et al.*, 2008; *Pacor et al.*, 2011]. Moreover, a novel approach for the assessment of the RAN performance as an EEWS at the national scale is proposed, which aims at both extending the feasibility analysis to regions that did not experience earthquakes over the last 10 years and considering the effective seismic hazard over the whole Italian territory.

2. The Italian Accelerometric Network

The Italian strong motion network, operated by and providing data to the DPC, consists of about 500 digital strong motion stations with data telemetry and time synchronization by GPS, with a 20–30 km mesh step, covering all the higher seismic hazard areas of Italy (Figure 1) and frequently placed in or nearby urban settings. All the data are collected, validated, and organized in the public database ITACA 2.0 [*Luzi et al.*, 2008; *Pacor et al.*, 2011].

The free field station data- loggers are mainly Etna or Basalt Kinemetrics with a high dynamic range (19–24 bits) and are equipped with three components FBA23 or Episensor sensors. The stations installed within the National Agency for Electric Energy (ENEL S.p.A.) substations are made up of Syscom motion processor units (www.syscom-instrument.com), REFTEK 130 data loggers, and FBA23 strong motion sensors. All the instruments have a ±1 g full-scale range, the time synchronization by GPS, and data telemetry by General Packet Radio Service (GPRS) digital data transmission. Presently, the RAN stations operate in a threshold trigger mode (i.e., after that the 10^{-3} g threshold is exceeded, the event recording begins, and it stops when the ground motion amplitude is equal to the preevent level). Then the waveforms are sent by GPRS to the DPC center. During an earthquake, the only information that is transmitted in real time from RAN stations to DPC by SMSs (short message services) are the PGA (Peak Ground Acceleration) values and the timing of the seismic event for a very rapid estimate of the ground shaking level. The RAN data center, placed in the DPC headquarter (Rome, Italy), controls the network efficiency and the strong motion data production by the software package "Antelope," provided by Boulder Real Time Technologies (http://www.brtt.com).
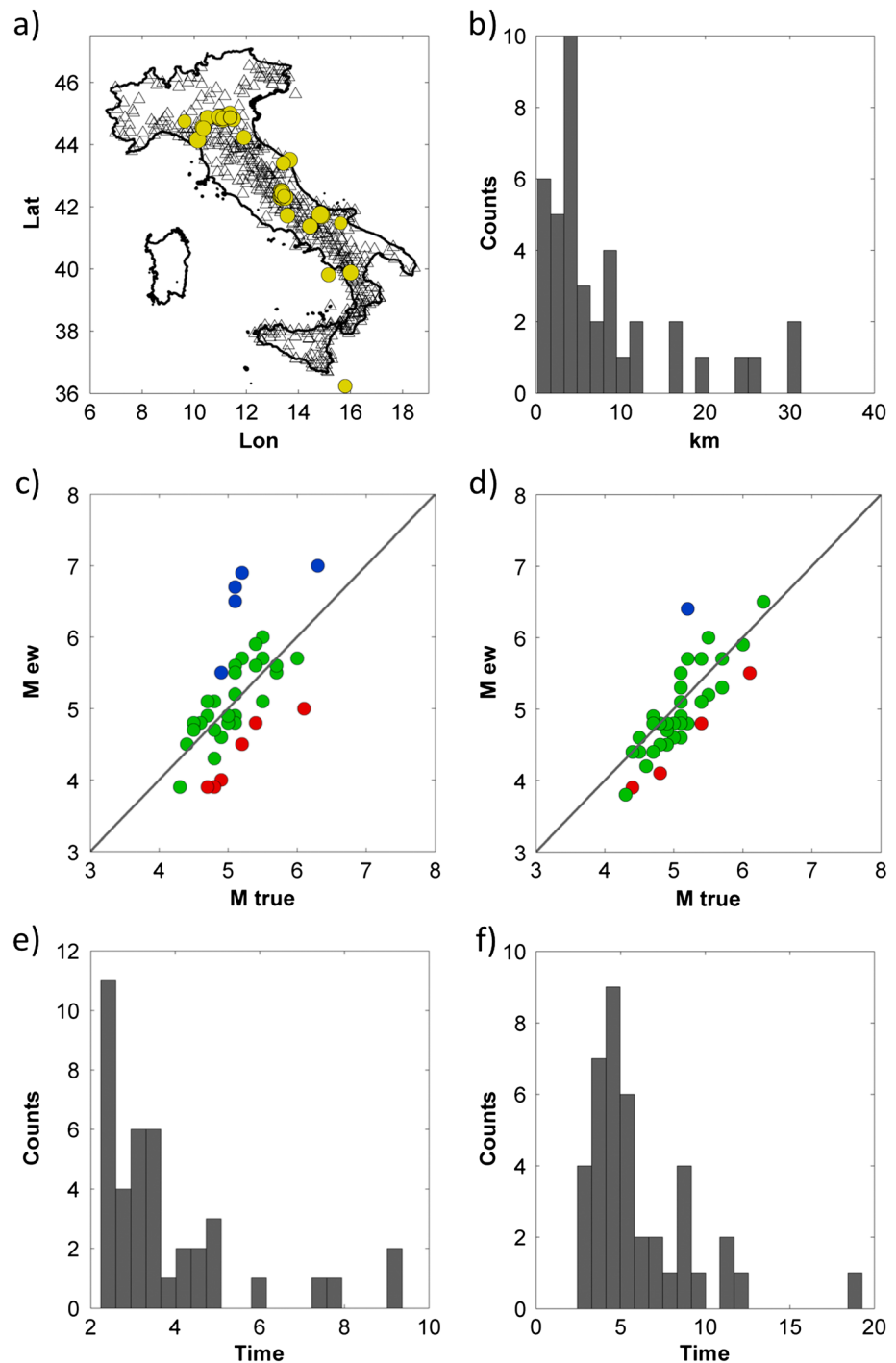
Figure 3. Results of the PRESTo playbacks with RAN recordings of 40 earthquakes having magnitudes larger than 4.5 that occurred in Italy during the period 2002–2013. (a) RAN stations (triangles) and epicenters (yellow dots). (b) Error in epicentral estimation. (c) Comparison of magnitude values estimated within the early warning timeframe M_{ew} (i.e., when three stations have triggered) and from bulletin, M_{true}: difference within 0.5 units (green), M_{ew} larger than M_{true} plus 0.5 unit (blue), M_{ew} less than M_{true} minus 0.5 units (red). (d) Same as Figure 3c but at the instant when the uncertainty associated with M_{ew} is less than 0.5 units. (e) Seconds needed by the PRESTo system for the first M_{ew} estimation. (f) Same as Figure 3e but for the instant when the uncertainty associated with M_{ew} is less than 0.5 units.

This work considers the RAN at its status as of February 2013, consisting of 309 free field stations and 194 stations deployed inside the ENEL electric transformer substations, for a total of 503 stations.

3. The Probabilistic and Evolutionary Early Warning System

PRESTo is a free and open source, highly configurable, and easily portable platform for EEW [*Iannaccone et al.*, 2009; *Satriano et al.* 2011]. PRESTo operates as both a *P* wave based, regional, and on-site system and integrates these two approaches into a procedure termed the "threshold-based method" [*Zollo et al.*, 2010, 2014], where the real-time mapping of a Potential Damage Zone is obtained. In the present study, we considered only the PRESTo regional component, and we leave to future studies the evaluation of performances of the on-site and the threshold-based methods.

The system processes the live accelerometric data streams from the stations of a seismic network to promptly provide probabilistic and evolutionary estimates of the location and magnitude of detected earthquakes while they are occurring, as well as the ground shaking predictions at the regional scale (Figure 2). The alarm messages containing all relevant earthquake parameters can reach target sites before the arrival of the destructive *S* and surface waves, so as to enable automatic safety procedures to be implemented.

In its regional configuration, PRESTo uses (a) a phase detector and picker algorithm, which is optimized for real-time seismic monitoring and EEWS [*Lomax et al.*, 2012]; (b) a location algorithm, RTLoc [*Satriano et al.*, 2008], which locates earthquakes using information from both triggered and not-yet-triggered stations and provides a fully probabilistic description of the hypocenter coordinates and origin time; (c) the RTMag algorithm [*Lancieri and Zollo*, 2008], a Bayesian approach that uses the peak displacement (Pd) measured on the first seconds of the high-pass-filtered signal on short time windows of P waves (i.e., 2 and 4 s) and *S* waves (i.e., 1 or 2 s), and empirical correlation relations between this parameter and the final earthquake magnitude (*M*); (d) finally, a ground motion prediction equation (GMPE) that allows the estimation of the peak ground motion at target sites (e.g., cities, infrastructures, and other seismic stations) using EW location and magnitude estimates.

In this work, we used the coefficients of the log(Pd) versus Magnitude relationship estimated by *Lancieri and Zollo* [2008] using the *European Strong-Motion Database* and the *Japanese K-Net/Kik-Net strong motion network data set*. Since our concern is on the performance of an EEWS in Italy for the case of strong events, the *Akkar and Bommer* [2007] GMPEs, derived from strong motion records of 131 earthquakes that occurred in Europe and the Middle East with moment magnitudes ranging from *Mw* 5 to 7.6, was adopted. PRESTo has been recently released to the scientific community (www.prestoews.org).

4. Principles and Methodologies of EEWS Performance Assessment

The procedures adopted in this study for assessing the potential of a nationwide EEWS in Italy provided by the integration of the RAN network and the PRESTo software can be grouped into two families: the first includes strategies based on the use of real data; in the second, analyses based on the use of synthetic data are gathered.

4.1. Performance Based on Real Data Analyses

The analyses based on real data consisted of the selection of RAN recordings and the realization of off-line runs of the PRESTo algorithms on earthquake waveform data (i.e., playbacks) from moderate events that occurred in Italy during the last decade. The selection of data was carried out using ITACA 2.0 [*Luzi et al.*, 2008; *Pacor et al.*, 2011], through which the RAN recordings are made freely available. We focused on the most recent data and selected RAN recordings of 40 earthquakes having magnitudes larger than 4.5 that occurred in Italy during the period 2002–2013 (Figure 3a).

In this case, the performance of the RAN-PRESTo system for early warning purposes was assessed in terms of its capability to provide the following: (1) the epicentral location, (2) the magnitude, and (3) the time with respect to the first *P* wave arrival at which the information about (1) and (2) are made available. Furthermore, due to the existence of an ineluctable trade-off between the number of recordings (i.e., stations) used for the early warning analysis, the precision of the early warning estimates, and the time when the warning is released, we decided to assess the system performance at two different instants: (1) when only three stations have triggered, which, from experience, we consider in most situations to be a good compromise between

Table 1. Characterization of the Seismic Sources Corresponding to the ZS9 Seismic Zonation [*Meletti et al.*, 2008], According to *Barani et al.* [2009][a]

Zone	M_{min}	M_{max}	ν	b	Z_{eff}
901	4.3	5.8	0.045	1.133	8
902	4.3	6.1	0.103	0.935	10
903	4.3	5.8	0.117	1.786	9
904	4.3	5.5	0.050	0.939	7
905	4.3	6.6	0.316	0.853	8
906	4.3	6.6	0.135	1.092	8
907	4.3	5.8	0.065	1.396	8
908	4.3	5.5	0.140	1.408	10
909	4.3	5.5	0.055	0.972	10
910	4.3	6.4	0.085	0.788	10
911	4.3	5.5	0.050	1.242	8
912	4.3	6.1	0.091	1.004	7
913	4.3	5.8	0.204	1.204	13
914	4.3	5.8	0.183	1.093	13
915	4.3	6.6	0.311	1.083	8
916	4.3	5.5	0.089	1.503	6
917	4.3	6.1	0.121	0.794	7
918	4.3	6.4	0.217	0.840	13
919	4.3	6.4	0.242	0.875	8
920	4.3	5.5	0.317	1.676	6
921	4.3	5.8	0.298	1.409	7
922	4.3	5.2	0.090	1.436	13
923	4.3	7.3	0.645	0.802	8
924	4.3	7.0	0.192	0.945	6
925	4.3	7.0	0.071	0.508	4
926	4.3	5.8	0.061	1.017	4
927	4.3	7.3	0.362	0.557	9
928	4.3	5.8	0.054	1.056	13
929	4.3	7.6	0.394	0.676	13
930	4.3	6.6	0.146	0.715	13
931	4.3	7.0	0.045	0.490	10
932	4.3	6.1	0.118	0.847	13
933	4.3	6.1	0.172	1.160	10
934	4.3	6.1	0.043	0.778	10
935	4.3	7.6	0.090	0.609	13
936	3.7	5.2	0.448	1.219	3

[a]For each zone the following information is provided: minimum (M_{min}) and maximum magnitude (M_{max}), annual rate of earthquake occurrence for M_{min} (ν) and negative slope of the Gutenberg-Richter relationship (b), and the "efficient depth," e.g., the bottom depth of the crustal layer within which the frequency distribution of the events is considered uniform (Z_{eff}). See Figure 4 for the distribution of the zones.

the necessity of optimizing the lead time and obtaining a reasonably well-constrained earthquake location and (2) when the evolutionary magnitude estimation is associated with an uncertainty interval less than ±0.5 magnitude units, which we consider, as a first approximation, an indication that the EEWS has reached a stable estimation. It is worth noting that the second performance criterion is done automatically and at different instants for each event, depending essentially on the network's geometry (i.e., the number and distribution of stations available at each instant) and the quality of the data.

4.2. Analyses Using Synthetic Data

In order to extend our analysis to the whole national territory and considering potentially damaging events (e.g., with magnitude $M > 6.5$), we decided to perform an extensive evaluation of the RAN-PRESTo system based on synthetic simulations. To this purpose, we discretized the whole country using the same grid adopted by the INGV (i.e., a node each $0.05° \times 0.05°$ for a total of 16,921 nodes) to derive the seismic hazard map in Italy (http://esse1-gis.mi.ingv.it/s1_en.php) and which is used in the Italian seismic code [*CS.LL.PP.*, 2008] (Figure 1). Each node of the grid has been considered as the virtual location of a seismic source capable of generating a ground motion equal to the maximum estimated for the seismic zones (ZSs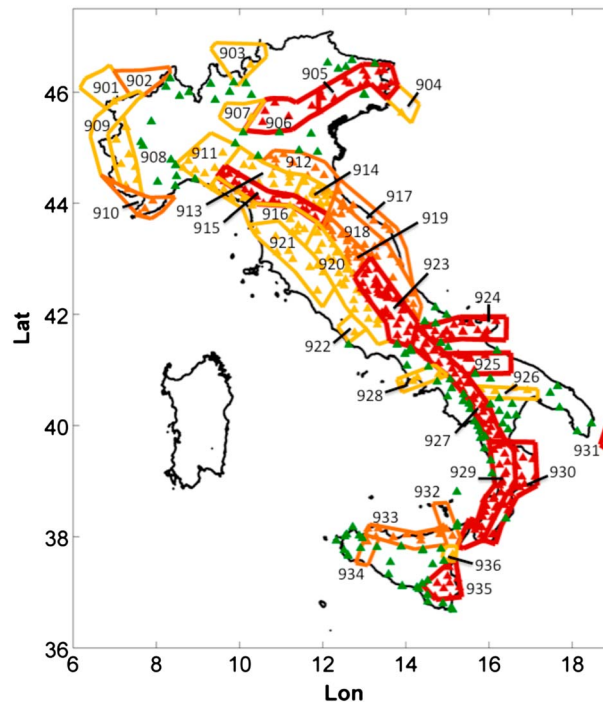) to which it belongs. We considered the ZS9 seismogenic zonation [*Meletti et al.*, 2008] and the seismic parameters of each zone as derived by *Barani et al.* [2009] and reported in Table 1. Despite the identified ZS for Italy numbering 42, six of them do not give a significant contribution to the seismic hazard of Italy [*Iervolino et al.*, 2011] and hence were not considered in this study. Furthermore, for each ZS, a seismogenic layer was defined as the depth interval where 90% of the events occur. This is named the "efficient depth," e.g., the bottom of the crustal layer within which the frequency distribution of the events is considered uniform [*Gruppo di lavoro MPS*, 2004, Table 1]. Then the ZS and the nodes representing the synthetic seismic sources were gathered into four classes (hereinafter, termed Macro Zones, MZs) based on the maximum magnitude expected for each ZS (Figure 4). In particular, in order of importance, the four MZs are as follows: (I) ZS with $M_{max} \geq 6.5$; (II) ZS with $6.5 > M_{max} \geq 6$; (III) ZS with $6 > M_{max} > 5$; and (IV) the nodes that do not belong to the previous ZS, and for which we assigned M_{max} equal to 5. Therefore, in the following sections, the results will be shown and discussed aggregated for the four MZs.

4.2.1. Network Geometry Criteria

The stations' distribution has a key role in determining the effectiveness of any EEWS, that is, to say the rapidity of the network in issuing an alert. As first parameter, we measured the network's performance

Figure 4. Distribution of RAN stations in the seismic macro-zones (MZs). These MZs are obtained by gathering seismic zones (ZS) with $M_{max} \geq 6.5$ (red); with M_{max} between 6 and 6.5 (orange); M_{max} between 6 and 5 (yellow); and finally, RAN stations outside of all ZS (green), which have been assigned to the fourth MZ. The numbers refer to the ZS listing in Table 1, according to *Barani et al.* [2009].

as the timing of the first alert, defined as the time when *P* waves reached a fixed number of stations (e.g., generally from three to six). This analysis has been carried out for each grid node using the four velocity models for the Italian region proposed by *Li et al.* [2007]. The EEWS performance of the RAN, as represented by the time of the first alert, therefore reflects mainly its geometrical characteristics.

The second parameter that we have used to characterize the EEWS performance is the extent of the blind zone (BZ). The BZ represents the region where no lead time is available (i.e., the lead time is zero or negative, meaning that the destructive *S* and surface waves reach the target site before an alert is issued) and no safety actions can be therefore undertaken. Differently from the time of the first alert, the BZ is related not only to the network's geometry but also to the operational procedures (i.e., telemetry, computation, and EW algorithm). In this study, we have defined the BZ as related to the sum of three delays: (1) the time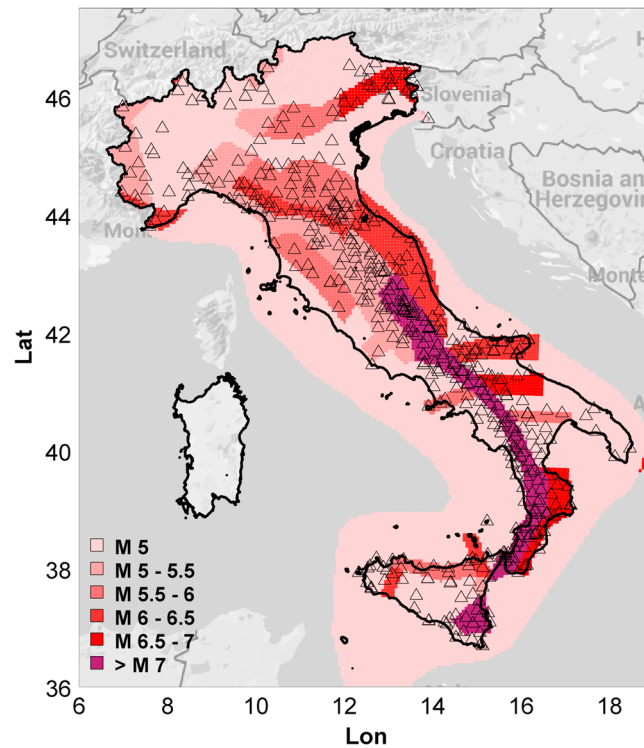 of the first alert, (2) a fixed delay for the telemetry and computation equal to 2 s, selected according to the value recorded with PRESTo at the ISNet accelerometric network in Southern Italy over a long period of testing [*Satriano et al.*, 2011], and (3) the constraint of having 2 s long *P* waves time windows at a N-1 stations used by RTLoc, which is the needed information for RTMag to estimate the magnitude. This latter constraint is due to the fact that at the instant when RTLoc locates an event with N stations, RTMag provides the first magnitude estimation using N-1 stations, under the condition that they recorded at least 2 s of *P* waves.

Finally, the sum of these three times is converted in the radius of BZ by multiplying it for the average *S* wave velocity as inferred by the velocity models proposed by *Li et al.* [2007].

4.2.2. Network Geometry and Reference Scenario Criteria

Taking into consideration the ZS proposed by *Meletti et al.* [2008] and the seismic parameters of each ZS proposed by *Barani et al.* [2009], we defined for each grid node a reference earthquake as the event having a magnitude corresponding to the 10% probability of occurrence in 50 years (Figure 5). For those nodes that were not included in any ZS, we forced the magnitude to be equal to 5. This set of large earthquakes gave us the possibility of assessing the performance and utility of a nationwide EEWS against a threat selected with a similar principle to the one used by the legislator to define the reference ground motion threat within the Italian seismic building code.

Figure 6 shows a simple conceptual scheme of the parameters we derived for quantifying the benefit/efficiency of an EEWS in Italy. In particular, for each node, the BZ area and an estimation of the "damage area" (DA) are compared. The latter, in particular, is defined as the area within which the peak ground velocity (PGV) is greater than 6.1 cm/s, which corresponds to the lower bound of the European Macroseismic Scale Intensity class VII [*Faccioli and Cauzzi*, 2006; *Grünthal*, 1998]. The selection of this Intensity class' lower bound provides the maximum possible extension of the damage area and is driven by the need to minimize the number of missed alerts, while we are aware that this comes at the price of potentially higher rates of false alerts. The selected PGV threshold is computed considering the reference earthquake assigned to the node itself and the *Akkar and Bommer* [2007] GMPE relationship. In order to take into account the variability of PGV values observed in

Figure 5. Magnitude values corresponding to the 10% probability of occurrence in 50 years with respect to which the EEWS RAN-PRESTo is tested.

experimental data, we defined three different DA values, which correspond to the average PGV, and this value plus and minus 1 standard deviation (σ) of the GMPE's predicted value. Whenever the DA is larger than the BZ, the area corresponding to a ring of finite thickness dR (given by the difference between the radii of DA and BZ) is characterized by a lead time greater than zero and is thus defined as the "Early Warning Zone" (EWZ). Of course, within an EWZ, the lead time ranges between 0 s at the BZ outer and a variable maximum value that is a function of the DA area size. We note that for the effective implementation of protective measures within the EWZ with the aim to reduce human losses, injuries, and damages, the lead time should be larger than the time necessary for the execution of the protective measures themselves and the time for the alert delivery. Concerning the transmission of the alert messages, which have typically the size of few tens of kiloby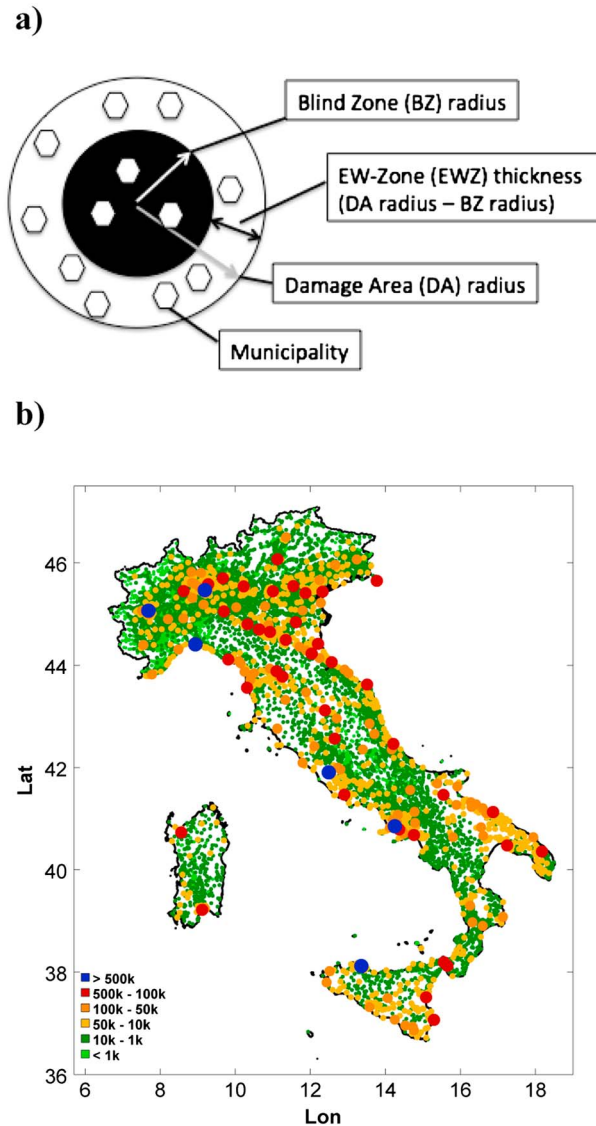tes, we measured at the ISNet network a latency of only a few tens of milliseconds [*Satriano et al.*, 2011]. On the contrary, the time required for the execution of protective measures is strongly user dependent and situation dependent, being influenced by the level of training and education of the users, as well as by the level of automation of security procedures. Although this aspect is beyond the scope of our study, we point out that it is crucial for establishing the effectiveness of an operational EEWS.

Finally, given the EWZ associated to a node, we also estimated the number of municipalities falling within it that potentially could receive an EW alert message from the RAN-PRESTo EEWS.

4.2.3. Gutenberg-Richter Derived Sequences

The last part of the performance analysis focused on the capability of the RAN-PRESTo EEWS to estimate the earthquake location and magnitude using only the data from a small number of stations (i.e., the operational condition of an EEWS). The analysis was carried out considering the grid of synthetic sources covering the whole country. In order to test the algorithm RTLoc applied to the RAN, we have computed first 10 sets of synthetic P wave arrival times for each node of the source grid,. These data have been created using the four velocity models for P and S waves derived for Italy by *Li et al.* [2007]. Moreover, two random sources of uncertainty have been added to the data: (1) a random error for each layer of the velocity models considering their uncertainty estimated by *Li et al.* [2007] and (2) a random noise around the estimated arrival time distributed according to a Gaussian distribution with standard deviation of 1 s. Therefore, by these large data sets, the RTLoc performance is assessed in terms of its capacity to estimate the epicentral location of the events.

Then, the RTMag algorithm was applied using simulated synthetic data. The seismogenic activity of each source was determined by the seismic hazard parameters of the ZS it belongs to. For each grid node, 10 earthquake sequences were generated, using a regular step of 0.5 magnitude units, following the Gutenberg-Richter (GR) frequency-magnitude distribution, over a virtual testing period of 50 years and M_w ranging between 5 and the maximum value associated to the ZS (i.e., M_{max} in Table 1). For each source, random samples of the peak displacement (Pd) at each of the first three triggered stations in terms of 2 s/4 s P and 2 s S waves are extracted from the log(Pd) versus M relationships proposed by *Lancieri and Zollo* [2008], along with the uncertainty

Figure 6. (a) Schematic representation of the parameters adopted for quantifying the PRESTo-RAN EEWS performance. (b) Municipalities and the relevant 2011 postcensus resident population in thousands (http://demo.istat.it).

bounds on empirical regression coefficients. By taking into account the uncertainties in the Pd-*M* relationships and in the real-time earthquake location, our simulated data reproduced the observed variability of observed *P* wave peak displacement measurements. A quantitative assessment of the RTMag performance in estimating the EW magnitude (M_{EEW}) was carried out by counting the success of the system, defined as the percentage of the total number of trials of M_{EEW} estimates falling within a ±0.5 interval around the true M_w.

5. Application and Results

In the following sections, we present the results from the application of the above procedures.

Figure 4 shows that the stations' density is much higher for the group of ZS with a seismic hazard larger than the others. This is not surprising, considering that the RAN was designed and developed throughout the years to cope with the past and actual seismicity distribution. We found that within the highest seismic hazard zone, MZ I (Figure 4), the station distribution is one per 308 square km (i.e., corresponding to an average interstations distance of about 17.6 km), which is a value similar to that of the Japan accelerometric network (i.e., average interstations distance of about 19 km). The other MZs show a station density of one every 544, 622 and 1134 square km (i.e., average interstations distance equal to 23.3, 24.9, and 33.7 km) for MZs II, III, and IV, respectively.

5.1. Performance of PRESTo and RAN on Real Data

Playbacks of real RAN earthquake waveforms were run offline in PRESTo for 40 earthquakes having magnitudes between 4.3 and 6.3 and that occurred in Italy during the period 2002–2013 (Figure 3a). Figure 3b shows that for most of the analyzed earthquakes, the RAN is so densely spaced that soon after three stations have triggered, the earthquake location is estimated within a distance less than 10 km from the location provided in ITACA 2.0. As for the first magnitude estimation, we observe that PRESTo, while relying on three stations only, provides a significant overestimation (e.g., a false alarm) of the ITACA bulletin moment magnitude (i.e., $M_{EW} > M_{w\text{-bull.}} + 0.5$ units) only in five cases out of 40 (i.e., 12.5% of the total). A magnitude underestimation (e.g., a missed alarm) is observed only for six cases (i.e., 15% of the total) for which $M_{EW} < M_{w\text{-bull.}} - 0.5$ units (Figures 3c and 3e). In the remaining 29 cases (i.e., 72.5%) the first reliable magnitude estimates (i.e., M_{EW} within the ±0.5 units of $M_{w\text{-bull.}}$) are provided within 2–3 s after the first *P* wave arrival. It is worth noting that these estimations were obtained by the off-line run of the PRESTo code, and they did not include the time necessary for data telemetry, which is here assumed to be 1 s as measured from the ISNet network.
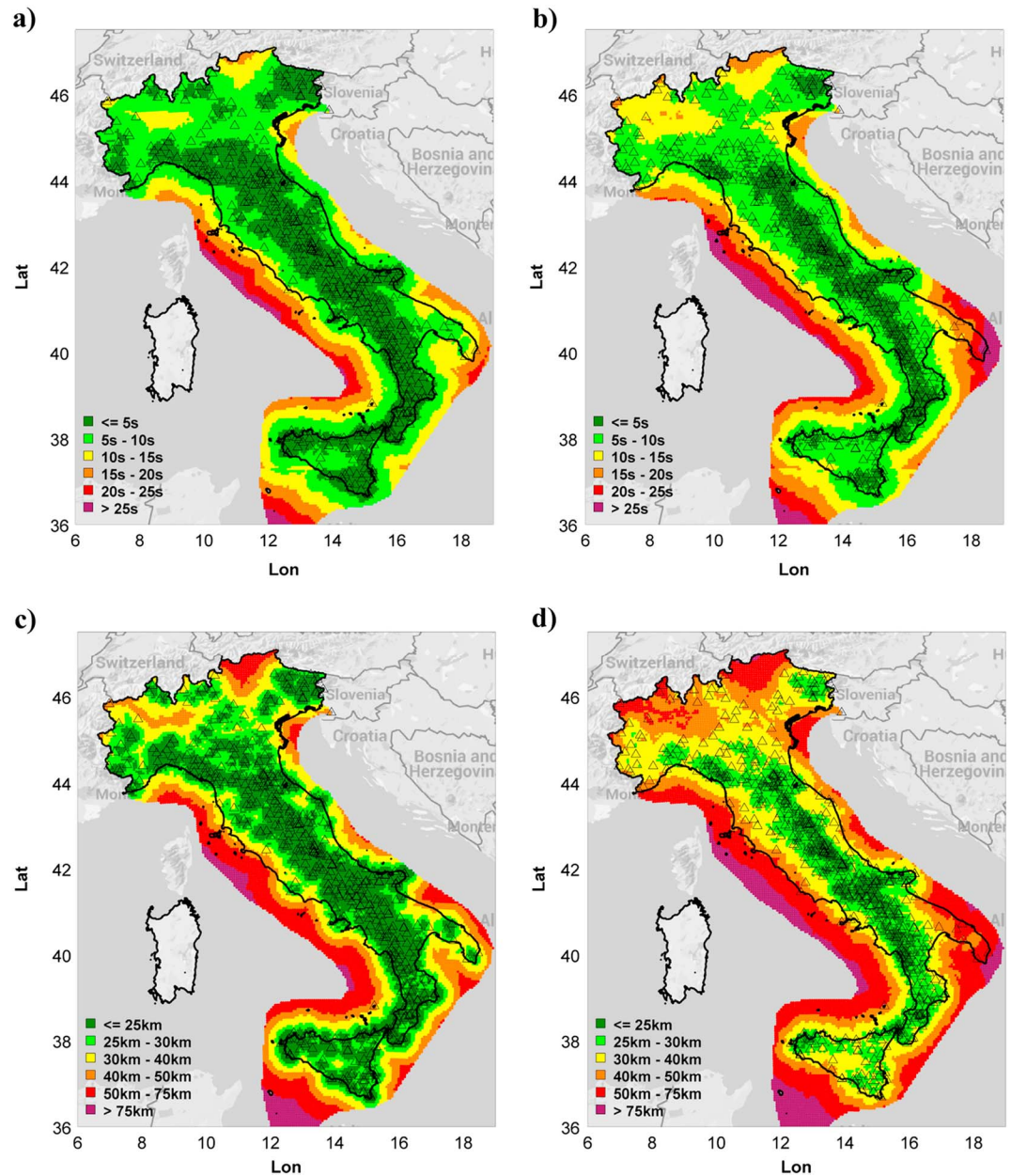
Figure 7. Distribution of the times of the first alert and radii of the blind zone for the grid of synthetic sources derived from the PSHA map for Italy. (a and b) Times of the first alert for three and six RAN stations triggered, respectively. (c and d) Same as Figures 7a and 7b but for the blind zone radii.

Table 2. Average of the EEWS Performance Parameters for the Four MZs and a Different Number of Triggered Stations[a]

Parameter	Number of Stations	I	II	III	IV
Time first alert (s)	3	3.7	4.5	5.0	11.4
Time first alert (s)	6	5.3	6.4	7.1	14.3
BZ radius (km)	3	23	25	26	42
BZ radius (km)	6	29	32	34	52

[a]Time is estimated off-line and does not include that needed for telemetry and computation.

Figures 3d and 3f show that waiting for a further 2–3 s (i.e., 5–6 s in total from the first P wave arrival) allows for the addition of more stations to the analysis, which in turn leads to a reduction of the number of false and missed events to one (i.e., 2.5%) and four (i.e., 10%), respectively, and a general convergence of M_{EW} estimates
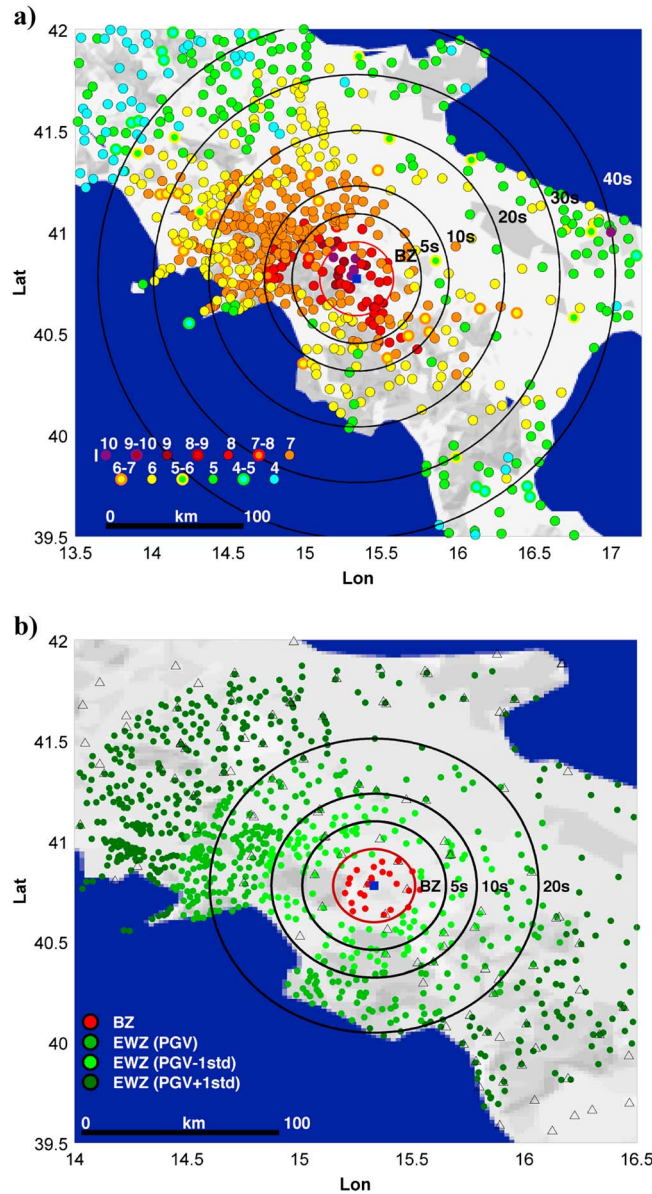
Figure 8. (a) Macroseismic intensity of the 23 November 1980 Irpinia Earthquake (M_w 6.9) from *Guidoboni et al.* [2007] (data available from *Locati et al.* [2011]). Epicenter (blue square), the circles indicate the BZ (red line) and distribution of LT (i.e., 5, 10, 20, 30, and 40 s, black line). (b) Municipalities within the BZ (red) and the EWZ (different green tone for the average PGV, and ±1 standard deviation, corresponding to the macroseismic intensity of level VII) for three triggered stations and the scenario mimicking the South Italy 1980 Irpinia Earthquake (M_w 6.9). LT circles are the same as in Figure 8a.

(i.e., 87.5%) toward values closer to the $M_{w\text{-bull}}$.

5.2. First Alert Time and Blind Zone

The influence of the station distribution on EEWS performance has been assessed considering the first alert time and the blind zone size for the cases of three and six triggered stations. Figure 7a shows that in the case where only three stations are considered, the first alert time is less than 5 s for most of the synthetic sources along the Apennine chain (i.e., the mountain range that extends along most of the Italian peninsula). The average values of this parameter for the four MZs are reported in Table 2 and range from a minimum of 3.7 s for MZ I (higher seismic hazard) to a maximum of 11.4 s for the nodes not included in any seismic zone (MZ IV). On the other hand, when six stations are considered (Figure 7b), the first alert time ranges from 5.3 to 14.3 s for MZs I and IV, respectively (Table 2). In the case where more stations are considered, the EW performance does not change significantly for most of the ZSs along the Apennine chain, and the first alert time remains around 5 s, thanks to the high station density. On the other hand, for parts of Sicily and Northeast Italy, also characterized by a high seismic hazard, we observe a worsening of the EW performance with the first alert time reaching values between 5 and 10 s (compare Figures 7a and 7b).

Figure 7c shows that when the EEWS is carried out using only three stations, the BZ has a radius less or equal to 25 km for most of the ZSs with a higher seismic hazard, and it is in general less than 40 km, with the exception of

Table 3. EEWS Performance for the 1980 Irpinia Scenario

Region	BZ (km)	EWZ (km) Mean PGV (−σ; +σ)	LT (s) Mean PGV (−σ; +σ)	N. Mun. BZ	N. Mun. EWZ Mean PGV (−σ; +σ)
Irpinia	20	56 (25; 110)	18 (8; 36)	31	414 (124; 847)

Table 4. Average of the EEWS Performance for the Four MZs Obtained Considering for Each Grid Node a Magnitude Having a 10% Probability of Occurrence in 50 Years

Parameter	Number of Stations	MZ I Mean PGV $(-\sigma; +\sigma)$	MZ II Mean PGV $(-\sigma; +\sigma)$	MZ III Mean PGV $(-\sigma; +\sigma)$	MZ IV Mean PGV $(-\sigma; +\sigma)$
EWZ width (km)	3	85 (41; 150)	2 (<0; 24)	<0	<0
EWZ width (km)	6	77 (36; 144)	<0 (<0; 17)	<0	<0
Lead time (s)	3	26 (13; 47)	<0 (<0; 8)	<0	<0
Lead time (s)	6	24 (11; 46)	<0 (<0; 5)	<0	<0
N. Municip.	3	493 (226; 915)	None (None; 89)	None	None
N. Municip.	6	472 (205; 894)	None (None; 69)	None	None

two areas in the Alps region (Northern Italy). The BZ radii associated with the four MZs are listed in Table 2 and range between 23 and 42 km for the zones I and IV, respectively. The performance of the RAN in terms of the BZ extent clearly worsened for the case when six stations are considered (Figure 7d). In fact, in this situation, only a few areas still have a BZ radius less than 25 km, although in most areas it remains less than 30 km, varying overall between 29 km and 52 km (Table 2).

5.3. EEWS Performance for Reference Earthquake Scenarios

Figure 8a shows the comparison between the BZ and the distribution of lead times for the scenario mimicking the 1980 Irpinia earthquake (*Ms* 6.9) [*Bernard and Zollo*, 1989] and considering the actual RAN configuration with respect to the observed macroseismic field after this event [*Guidoboni et al.*, 2007; *Locati et al.*, 2011, data available from http://emidius.mi.ingv.it/DBMI11/]. Keeping into consideration only the municipalities to which it was assigned a macroseismic intensity I_{MCS} equal or larger than VII (i.e., from moderate toward very high damage), and assuming that an EEWS was operational, we observe that 35 municipalities fell within the BZ; 53 had lead times (LT) less than 5 s; 73 had LT between 5 and 10 s; 112 had LT between 10 and 20 s; and finally, 24 had more than 20 s of LT. This example shows that an EEWS would have hypothetically provided an alert message to about 262 municipalities affected by damage, of which 136 would have benefited an LT larger than 10 s.

We extended a similar kind of EEWS performance analysis to all the grid nodes of Italy, using the reference earthquakes with 10% probability of occurrence in 50 years and the procedure described in section 4.2.2. In Figure 8b and Table 3 we present the damage area (DA), blind zone (BZ), and early warning zone (EWZ) extent considering three triggered stations for the 1980 Irpinia scenario. Given the actual high density of RAN stations in the Irpinia area, the estimated BZ is about 20 km, while the number of municipalities therein is 31 (Table 3). Despite few tens of municipalities falling within the BZ area, which could not have benefited of a regional EEWS, it is worth noting that the EWZ radius is 56 km, and 414 municipalities fall within it (Table 3 and Figure 8b). Comparing Figures 8a and 8b, it is worth noting that the number of municipalities with $I_{MCS} \geq$ VII is similar to one of municipalities included within the EWZ using the mean PGV values of the GMPE. According to this simulation, the maximum lead time for municipalities within the EWZ would be of 18 s (Table 3). On the other hand, considering the PGV + 1σ, which represents the worst case scenario, the number of municipalities within the EWZ grows to 847.

The results of the performance analysis for the whole Italian territory considering three and six triggered stations are reported in Table 4, while Figure 9 presents the results for the case of three triggered stations only. We observe that for the MZs II, III, and IV the EWZ radii and lead time are null. This is clearly due to the low maximum magnitude expected in these areas, which, given the current RAN geometry, would determine DA computed considering the mean PGV comparable to the BZ. Therefore, in moderate to low seismic hazard areas, the on-site EEWS strategies could be better suitable. On the contrary, in the higher seismic hazard areas (MZ I) the possible future occurrence of large magnitude events leads the EWZ radii and lead times always positive (Table 4), both considering three and six triggered stations. In particular, Figure 9 and Table 4 show that where the magnitude of the reference earthquake is larger than 6.5 (compare with Figure 5), the EWZ extent considering three triggered stations is on average about 85 km. This leads to maximum lead times larger than 25 s and the number of municipalities that potentially might receive a warning message equal to 493 (Table 4).
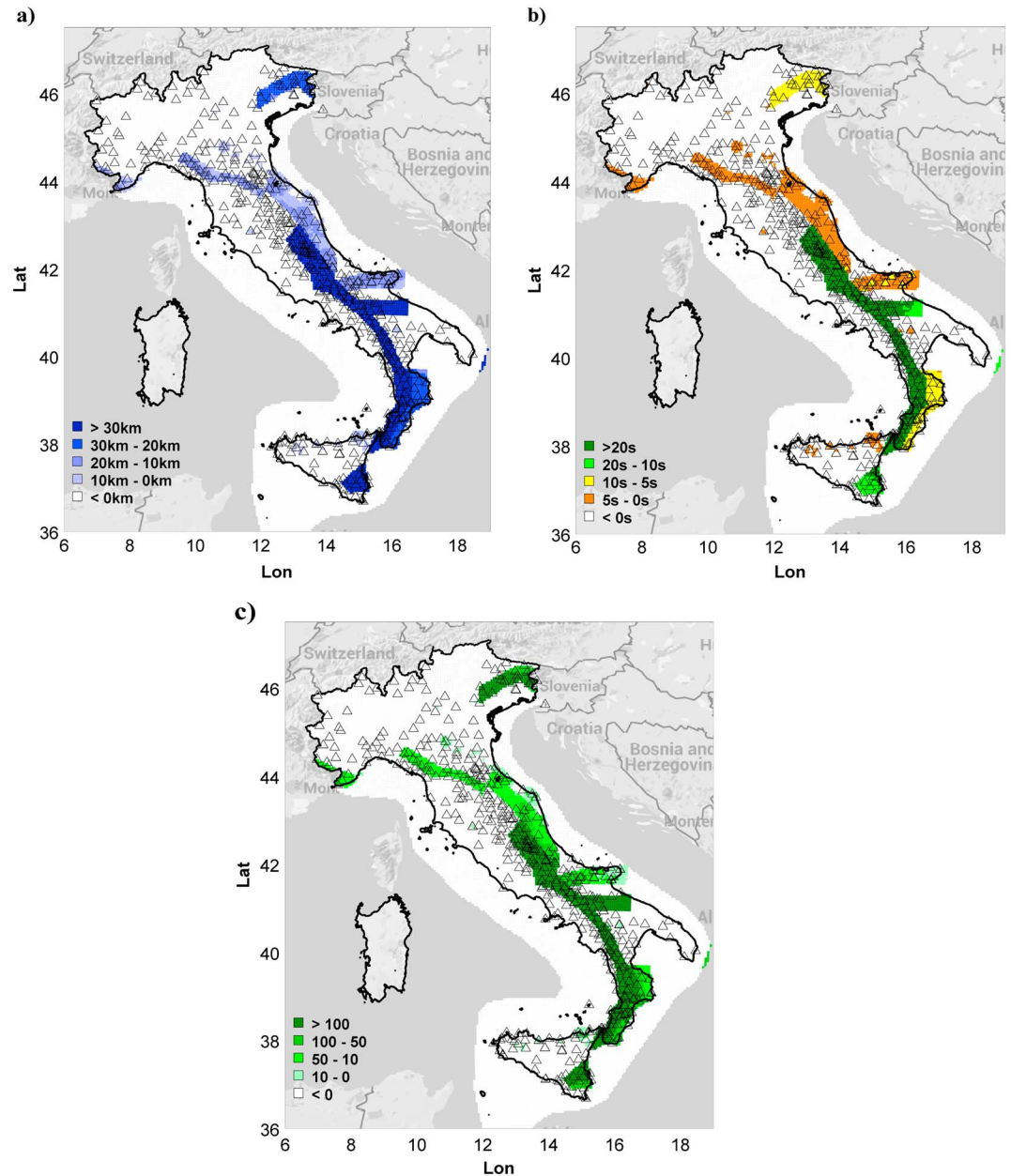
Figure 9. Overview of the EW parameter performance for reference events (i.e., with a magnitude > 5 having 10% probability of occurrence in 50 years) for three triggered stations: (a) Radius of the Early Warning Zone; (b) Maximum lead time; (c) Number of municipalities within the Early Warning Zone.

5.4. EEWS Performance in Estimating Earthquake Location and Magnitude

Figure 10 shows the average epicentral error obtained after 10 runs of RTLoc for each grid node, while Table 5 shows the same results grouped for the four MZs. The results indicate that, in both cases, location errors larger than 20 km are obtained only for offshore sources and a few, small, on-land areas, while the EW location can be associated with errors in the range 5 to 10 km for most of the Italian territory. These results are in good agreement with the location errors found using PRESTo on real RAN recordings (Figure 3b).

Figure 11 shows, as example, the performance of the RTMag algorithm for the 1980 Irpinia earthquake scenario using three triggered stations. In particular, Figures 11a and 11b show the *P* and *S* wave Pd samples randomly extracted from log(Pd) versus *M* relationships proposed by *Lancieri and Zollo* [2008] for 10 seismic
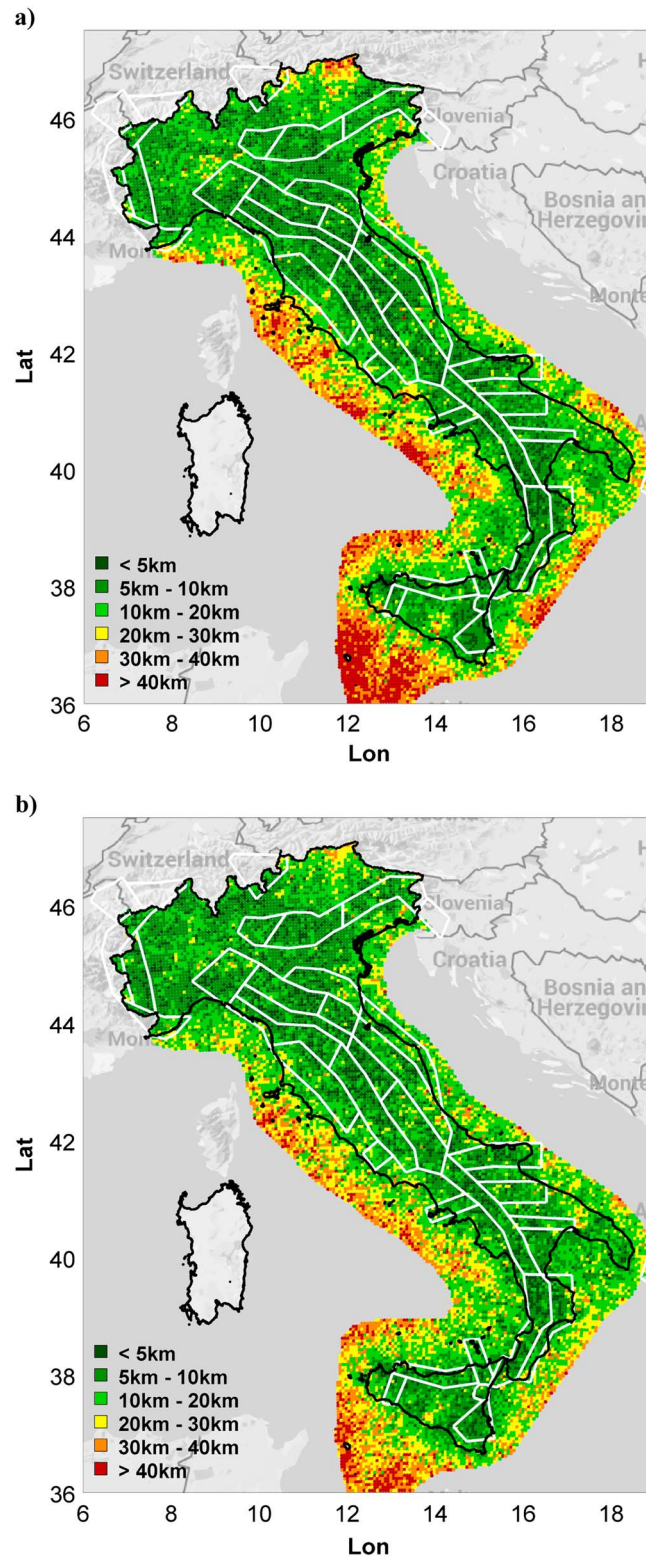
Figure 10. RTLoc performance on synthetic data at the national scale in terms of average epicentral error. (a) Three triggered stations and (b) six triggered stations. Boundaries of the ZS, are shown as white lines.

sequences. These data are, together with RTLoc event location, the input of the RTMag algorithm. The result of the analysis is shown in Figure 11c as the comparison between the true and EW estimated magnitudes. We observe that the RTMag estimates show only a small level of dispersion around the true magnitudes (e.g., within ±0.5 magnitude units and never exceeding ±1 magnitude unit), and no systematic bias affects the results. The same analysis was carried out on the grid of synthetic sources covering the whole country and considering both three and six triggered stations. Figure 12 shows the results of this analysis in terms of the percentage of success/failure in M_{EW} estimations. In general, the results indicate a high percentage of success (i.e., close or higher than 90% throughout most of the country), especially when six triggered stations are considered.

We observe that the RAN-RTMag performance for three triggered stations is not uniform throughout the different ZSs. Figure 12a shows rather low percentage of success (i.e., between 75% and 50%) for two areas in the Alps region (north Italy) and one area in Sicily (south Italy) where the RAN's density is low, as well as in the case of off-shore grid node where RTLoc provided large epicentral errors (see Figure 10). In addition, Figure 12c shows that where RTMag has the worst performance, missed alarms (i.e., $M_{EW} < M_{w\text{-bull.}} - 0.5$ unit) are more frequent than false alarms (i.e., $M_{EW} > M_{w\text{-bull.}} + 0.5$ unit). Hence, in these areas the RAN-RTMag system seems prone to underestimating the size of large magnitude events. However, it is worth noting the very good performance of the system in the regions with higher seismic hazard (compare Figures 1 and 12a). Table 6 summarizes the results of this analysis for the four MZs. In particular, for MZs I–III the RTMag's success rate is above the 95%, while it underestimates in average the magnitude (i.e., missed events) in ~2.5% of the cases, and overestimates (i.e., false events) in

Table 5. Average RTLoc Epicentral Errors (in km) for the Four MZs

Number of Stations	MZ I	MZ II	MZ III	MZ IV
3	8.1	9.	9.7	20.3
6	8.7	9.4	10.5	18.1

1–2%. On the contrary, within the MZ IV, the success, false, and missed are 71.5%, 2.6%, and 25.9%, respectively.

When six stations are considered, the RTMag performance slightly improves (compare Figures 12a and 12b). Figure 12b shows that the percentage of success is larger than 95% in most of the country. Similarly to Figure 12c, Figure 12d shows that in the areas where RTMag is less efficient, the magnitudes are in general underestimated. Table 7 provides the average percentage of success for the four MZs and shows the improvement in the EW magnitude estimation when more stations are considered. In fact, successful magnitude predictions range between about 98% and 85%, underestimations between 0.6% and 13%, and overestimations between 0.4% and 1.4%.

6. Discussion

The previous sections presented the results of analyses carried out by using real and synthetic data with the aim of assessing the scientific feasibility and performance of a nationwide earthquake early warning system in Italy based on the RAN network and the EW software platform PRESTo.

The performance analysis of the PRESTo regional scheme integrated with the RAN was limited to the estimation of earthquake location and magnitude. Despite the fact that predicting the ground motion severity at target sites is the final outcome of an EEWS, we decided not to include this issue in our performance assessment of the RAN-PRESTo system because such an analysis would mostly depend on the chosen GMPEs. Moreover, while most of the EEWS software, including PRESTo, implicitly adopts the point source assumption, in case of large magnitude events (i.e., $M > 6.5$), the finite extent of the fault must be properly accounted for, along with directivity effects and the source mechanism, all of which could have a dominant role on the ground motion at near-source target sites. A complementary approach, such as the threshold-based EW method proposed by *Zollo et al.* [2010, 2014] and *Colombelli et al.* [2012], would allow accounting, as a first approximation, for the source finiteness by directly mapping the Potential Damage Zone using the early P wave peak displacement and characteristic period measurements at the near-source stations.

The performance of a nationwide RAN-PRESTo EEWS was first assessed by playbacks of real data from 40 moderate earthquakes that occurred during the last 10 years in Italy and were recorded by the RAN. In particular, we evaluated the network capability of providing fast earthquake location and magnitude estimations, as well as the time after the first P wave arrival for which this information is made available. For the locations, our results indicate that when using only three triggered stations, the retrieved locations differ in most cases from the bulletin ones by less than 10 km. It is worth noting that considering the Pd-M
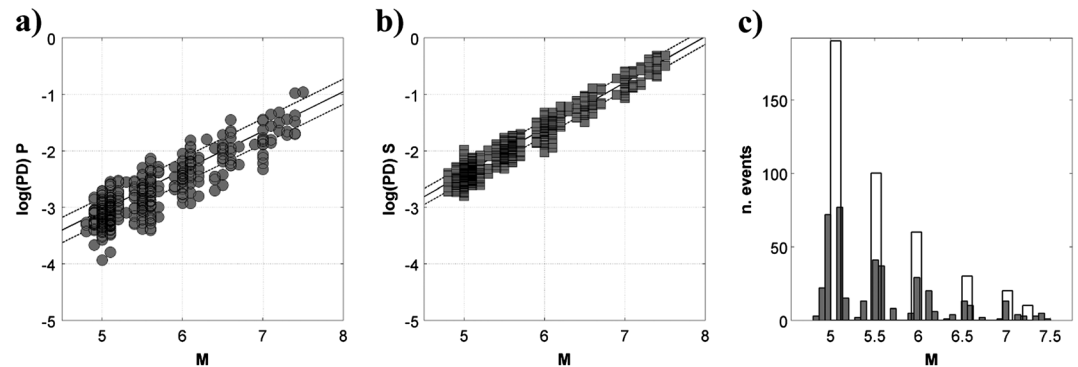

Figure 11. Results of the RTMag analysis on synthetics derived from the simulation of the seismicity related to ten 50 years sequences in the same area of the 1980 Irpinia Earthquake. (a) P waves displacement peaks for a 4 s time window (grey dots), Pd-M relationships proposed by *Lancieri and Zollo* [2006] ±1 standard deviation (black lines). (b) Same as Figure 11a but for S waves peak displacement in a 2 s window. (c) Histogram of the input (white bars) and output (gray bars) magnitude estimation.
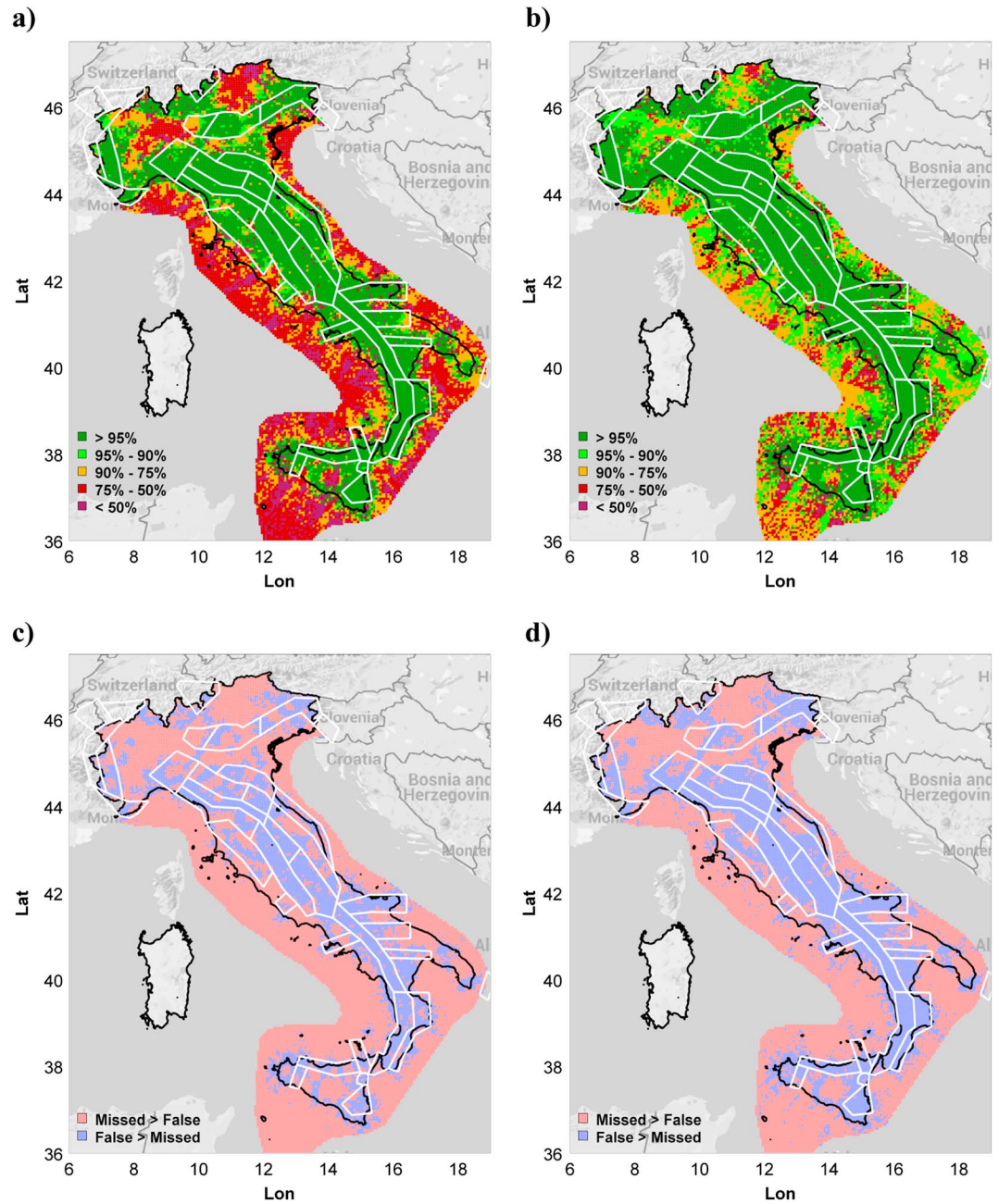
Figure 12. RTMag performance at the national scale from the simulation of ten 50 years long seismic sequences according to the Gutenberg-Richter parameters of the ZS: (a) percentage of success (i.e., M_{ew} included within the range $M_{true} \pm 0.5$ unit) for three triggered stations; (b) same as Figure 12a but for six triggered stations; (c) distribution of missed and false M_{ew} estimations for three triggered stations; (d) same as Figure 12c but for six triggered stations. Boundaries of the ZS are shown as white lines.

Table 6. Average Rtmag Success, False, and Missed Rates (in %) for the Four MZs in Case Three Stations Are Used

Performance	MZ I	MZ II	MZ III	MZ IV
Success	97.1	95.9	95.8	71.5
False	1.4	1.5	0.7	2.6
Missed	1.5	2.6	3.5	25.9

relationship proposed by *Lancieri and Zollo* [2008], location errors within 50 km correspond to errors in magnitude of less than 0.5 units. The magnitude estimation with three stations, which would be available within 3 to 4 s after the first *P* wave

Table 7. Same as Table 6 but for the Case of Six Stations

Performance	MZ I	MZ II	MZ III	MZ IV
Success	98.2	97.8	98	85.6
False	1.2	*1.2*	0.4	1.4
Missed	0.6	1	1.6	13

arrival, was successful, false, and missed in 72.5%, 12.5%, and 15% of cases, respectively. When a further 2 to 3 s of signal are used, allowing for more stations to be included in the analysis, successful, false, and missed rates change to 87.5%, 2.5%, and 10%, respectively. The analyzed strong motion data are relevant to some of the most historically active seismogenic Italian areas; thus, we believe they provide a clear indication that the integrated RAN-PRESTo EEWS might have, from this point of view, a great potential to issue a rapid alert after moderate to large earthquakes.

The analyses with synthetic data confirmed that the density of RAN stations in seismogenic zones has an important and direct impact on the EEWS performance, both in terms of geometrical and physical parameters of the source. Indeed, under the assumption of a fixed delay in the data telemetry and computation, we observed that the stations' distribution constrains the first alert time to be around 4 and 5.5 s in the high seismic hazard areas for the cases of three and six triggered stations, respectively. Furthermore, the blind zones in these areas have radii of about 25 and 30 km when three and six stations have triggered, respectively. Such dimensions of blind zones indicate that a regional EW approach, such as the one explored in this study, would provide lead times greater than zero only for events having magnitude larger than 6.5. These large threatening events, even if they occur less frequently than the smaller ones, are capable of generating great losses both in human and economic terms. For this reason, taking example from Japan and California, a country like Italy prone to large seismic hazard should employ all the existent seismic risk mitigation tools and strategies, including an EEWS.

The EEWS performance analysis that we have carried out, based on reference earthquake scenarios, indicates that for large earthquakes in the higher hazard zones, the EWZ sizes would be in the order of 80 km, the maximum lead time around 25 s, and the number of municipalities for which an alert would be useful in the order of 5 hundreds. These results are in agreement with the comparison between the macroseismic field after the 1980 Irpinia Earthquake and the LT that we theoretically estimated for this event considering the actual RAN geometry (Figure 8). In particular, we observe several tens of municipalities with $I_{MCS} \geq$ VII with the zone, with a LT between 10 and 40 s. Moreover, several hundreds of municipalities are within the zone that experienced I_{MCS} between V and VII. In this area, where the shaking perception was high, but no significant damages were observed, an EEWS's alert could be useful to inform the population about the impending earthquake, and mitigate the panic effect.

As for the network capability to provide fast and reliable estimations of earthquake location and magnitude using only three and six stations, our analyses indicate that (a) location errors larger than 20 km affect mainly offshore sources; (b) the combination of a dense seismic network such as the RAN and a robust location algorithm, as RTLoc in PRESTo, allows for EW locations with errors in the range between 5 and 10 km along most parts of the Italian territory; (c) location errors obtained from synthetic data analyses are in good agreement with those found running PRESTo playback on real RAN acceleration recordings; (d) with respect to the location errors obtained considering six stations, the use of only three stations apparently provides slightly better EEWS results, with the advantage of allowing also smaller blind zones (Figure 7). This last observation is confirmed by the average epicentral error of the MZs I, II, and III (Table 5). We consider these findings to be related to the stations' density and, in particular, to the use of both triggered and not triggered stations in RTLoc, together with the level of noise associated with the picks of the triggered stations. Indeed, where the RAN has a relatively high density, the availability of three noise-biased picks, combined with the existence of many nearby, not triggered stations, allows a more robust location estimate than the case when six noise-biased picks are used.

The performance analysis of the RAN-RTMag system shows that the use of both three and six stations led to a very high percentage of success (>95%) in estimating accurate location and magnitude, over most of the high seismic hazard areas throughout the country (Tables 6 and 7, Figures 12a and 12b). Our results indicate that if an integrated EEWS such as RAN-PRESTo would be operational, by using only the closest three stations to the epicenter, the moderate to large events potentially occurring in the greater part of the country could be rapidly detected (i.e., in less than 5 s) and sufficiently accurate estimations of location and magnitude

Table 8. Examples of Actions That Could Be Taken When Considering 10 s Warning Time (Modified From *Goltz* [2002])

Education: -Notify teachers with mobile phones -Shut off gas -Alert custodial staff to secure building -Shut off machines, move away from lab equipment -Notify security to be on alert -Get mobile phones -Move clear of potentially falling objects	Emergency Services: -Turn off computer -Send alert to fire department command center -Warn the community -Make sure everyone is out of elevators -Activate backup -Alert field workers -Shut down equipment -Evacuate bottom floor -Stop hazardous work -Secure equipment
Health Care: -Shut off equipment -Secure supplies -Secure patients -Shut off gas -Stop surgeon activities -Shut off water -Stop elevators	Utilities and Transportation: -Start automatic sms -Shut down computers -Shut down gas -Alert drivers -Control traffic signals -Put information on the computer

could be obtained (i.e., in more than 95% of the cases). If, for example, we consider the seismicity observed in the last 40 years in Italy (i.e., 67 events with $M > 5$ in the ITACA 2.0 database recorded during the period 1972–2013, of which nine had an M larger than 6), we expect that a RAN-PRESTo EEWS would be successful and capable of delivering useful warning with respect to about 63 of them (59 if we consider the 87.5% rate of success found by playbacks of PRESTo with RAN recordings of 40 earthquakes).

In areas with lower seismic hazard, the expected magnitude of the events is smaller (between 5 and 6) and the maximum extent of the potential damage area (i.e., $I_{MM} \geq VII$) is of the same size of the blind zone (i.e., lead time < 0). In these cases, two possible strategies can be followed: (1) to decrease the blind zone dimension by increasing the network density, (2) to integrate the EEWS with the on-site method. Although on-site single station analyses do not provide the earthquake location and magnitude estimates, the relationship between P peak ground motion (i.e., Pd, peak displacement; Pv, peak velocity, and Pa, peak acceleration) and the S wave ground shaking (PGV, PGA) is robust. Increasing the station density and adopting on-site EEWS strategies would therefore reduce the blind zone area and thus increase the extent of the early warning zone.

Considering the already high RAN density in the high hazard ZSs of Italy, if a long-term program for the implementation of a nationwide EEWS in Italy would start, in addition to upgrading the network to enable real-time data telemetry, as a first step we would suggest increasing the station density in areas classified at the moment with a lower seismic hazard, especially in northern Italy and in Sicily region, for which now we observed the worst EEWS performance.

In our approach the lead time estimate is based upon the first S arrival time as obtained from the earthquake location. However, we point out that this value likely underestimates the time available for automatic/individual security actions, since rarely first S arrivals are associated with the strongest ground shaking. Also, the failure of building structural/non structural elements may take some time and not be contemporary to the strong ground shaking. From the practical point of view, the effective implementation of a protective measure against the earthquake effects is possible only when the lead time is larger than the time required to execute the protective measure itself. The decade-long experience of an operational EEWS in Japan outlines the primary importance of the training and education of the EW users on the seismic risk and on the protective measures that could be taken within a few seconds after an EW alert. In particular, training exercises should be specifically tailored for the different users. Related to this topic, we mention two studies. The first is a study committed by the Governor's Office of Emergency Services in California aimed at defining, in agreement with users belonging to the institutional sector (i.e., education, health care, emergency response agencies of state and local government, and utilities and transportation lifelines), the actions that these organizations could take when a lead time of 10 s were available [*Goltz*, 2002] (Table 8). The second study is a pilot experimentation of an EEWS in Italy [*Picozzi et al.*, 2015], where it has been verified by drill tests that the protection of students at

schools (i.e., duck and cover before the *S* waves arrival) is among the possible actions to take in a relatively short time (<10 s; a video presenting the drill can be seen at http://www.rissclab.unina.it/en/experiments/710-early-warning-applicationa-at-school).

7. Conclusion

In this work, we explored the usefulness, reliability, and potential of an EEWS that combines a high quality, nationwide, strong motion network (RAN) and a software platform for alert management (PRESTo) able to perform robust real-time analysis of seismic data. Our study takes into account the geometrical configuration of the potential earthquake sources and actual receiver positions, real strong motion data, and hazard-based scenarios generated for the whole country. It does not include the EEWS operability, which asks for experimental testing and the close involvement of potential end users. Despite some simplifications and assumptions, the results of our simulation study suggest that a nationwide RAN-PRESTo EEWS can provide reliable alert messages within 5 to 10 s after the occurrence of a moderate to large earthquake. Maximum lead times of about 25 s are inferred for earthquakes generated in the higher seismic hazard zones. Therefore, an EEWS could potentially assist the population in taking basic protective measures (e.g., duck and cover, move away from windows or equipment) in tens to hundreds of municipalities affected by large ground shaking. On the contrary, given the lower efficiency of a regional EW approach in regions characterized by low seismic hazard, a further important step in EW operations would be to integrate the regional and a *P* wave, threshold-based on-site methods into an EW decisional platform [e.g., *Zollo et al.*, 2010]. An ongoing study on the feasibility of EEWS in Italy considering an integrated regional and on-site early warning system will investigate the performance of such an EW system.

Notation

EW	early warning.
EEWS	Earthquake Early Warning Systems.
RAN	Italian Accelerometric Network.
PRESTo	PRobabilistic and Evolutionary early warning SysTem.
ZS	seismic zone.
MZ	macro zone.
BZ	blind zone.
DA	damage area.
EWZ	early warning zone.

References

Akkar, S., and J. J. Bommer (2007), Empirical prediction equations for peak ground velocity derived from strong-motion records from Europe and the Middle East, *Bull. Seismol. Soc. Am.*, 97(2), 511–530.

Allen R. M. (2007), The ElarmS earthquake early warning methodology and its application across California, in *Earthquake Early Warning Systems*, edited by P. Gasparini, G. Manfredi, and J. Zschau, pp. 21–43, Springer, Berlin, doi:10.1007/978-3-540-72241-0_3.

Allen, R. M., and H. Kanamori (2003), The potential for earthquake early warning in Southern California, *Science*, 300, 786–789, doi:10.1126/science.1080912.

Allen, R. M., P. Gasparini, O. Kamigaichi, and M. Böse (2009), The status of earthquake early warning around the world: An introductory overview, *Seismol. Res. Lett.*, 80(5), 682–693, doi:10.1785/gssrl.80.5.682.

Barani, S., D. Spallarossa, and P. Bazzurro (2009), Disaggregation of probabilistic ground motion hazard in Italy, *Bull. Seismol. Soc. Am.*, 99, 2638–2661.

Bernard, P., and A. Zollo (1989), The Irpinia (Italy) 1980 Earthquake: Detailed analysis of a complex normal faulting, *J. Geophys. Res.*, 94(B2), 1631–1647, doi:10.1029/JB094iB02p01631.

Colombelli, S., O. Amoroso, A. Zollo, and H. Kanamori (2012), Test of a threshold-based earthquake early warning using Japanese data, *Bull. Seismol. Soc. Am.*, 102, 1266–1275, doi:10.1785/0120110149.

CS.LL.PP. (2008), DM 14.1.2008 Norme tecniche per le Costruzioni, Gazzetta Ufficiale della Repubblica Italiana 29 [in Italian].

Cua G., Heaton T. (2007), The virtual seismologist (VS) method: A Bayesian approach to earthquake early warning, in *Earthquake Early Warning Systems*, edited by P. Gasparini, G. Manfredi, and J. Zschau, Springer, Berlin, doi:10.1007/978-3-540-72241-0_7.

Doi, K. (2011), The operation and performance of earthquake early warnings by the Japan Meteorological Agency, *Soil Dyn. Earthquake Eng.*, 31(2), 119–126, doi:10.1016/j.soildyn.2010.06.009.

Faccioli, E., and C. Cauzzi (2006), Macroseismic intensities for seismic scenarios estimated from instrumentally based correlations, paper 569 presented at the First European Conference on Earthquake Engineering and Seismology (a joint event of the 13th ECEE & 30th General Assembly of the ESC), Genève, Switzerland.

Gasparini, P., G. Manfredi, and J. Zschau (2010), Earthquake early warning as a tool for improving society's resilience and crisis response, *Soil Dyn. Earthquake Eng.*, *31*(2), 267–270, doi:10.1016/j.soildyn.2010.09.004.

Goltz, J. D. (2002), Introducing earthquake early warning in California: A summary of social science and public policy issues, Tech. rep., Governor's Off. of Emergency Serv., Pasadena, Calif.

Gorini, A., M. Nicoletti, P. Marsan, R. Bianconi, R. De Nardis, L. Filippi, S. Marcucci, F. Palma, and E. Zambonelli (2010), The Italian strong motion network, *Bull. Earthquake Eng.*, *8*, 1075–1090, doi:10.1007/s10518-009-9141-6.

Grünthal, G. (1998), *European Macroseismic Scale 1998 (EMS-98)*, *Cah. Cent. Eur. Géodyn. Séismol.*, vol. 15, 99 pp., Centre Européen de Géodynamique et de Séismologie, Luxembourg.

Gruppo di lavoro MPS (2004), Redazione della mappa di pericolosità sismica prevista dall'Ordinanza PCM 3274 del 20 marzo 2003, Rapporto conclusivo per il dipartimento di Protezione Civile, INGV, Milano—Roma, aprile 2004, 65 pp. + 5 appendici, Internet web site. [Available at http://zonesismiche.mi.ingv.it/elaborazioni/.]

Guidoboni, E., G. Ferrari, D. Mariotti, A. Comastri, G. Tarabusi, and G. Valensise (2007), CFTI4Med, Catalogue of Strong Earthquakes in Italy (461 B.C.–1997) and Mediterranean Area (760 B.C.–1500). INGV-SGA. [Available at http://storing.ingv.it/cfti4med/.]

Iannaccone, G., et al. (2009), A prototype system for earthquake early-warning and alert management in southern Italy, *Bull. Earthquake Eng.*, doi:10.1007/s10518-009-9131-8.

Iervolino, I., E. Chioccarelli, and V. Convertito (2011), Engineering design earthquakes from multimodal hazard disaggregation, *Soil Dyn. Earthquake Eng.*, *31*, 1212–1231.

Kamigaichi, O., M. Saito, K. Doi, T. Matsumori, S. Tsukada, K. Takeda, T. Shimoyama, K. Nakamura, M. Kiyomoto, and Y. Watanabe (2009), Earthquake early warning in Japan: Warning the general public and future prospects, *Seismol. Res. Lett.*, *80*(5), 717–726, doi:10.1785/gssrl.80.5.717.

Kanamori, H. (2005), Real-time seismology and earthquake damage mitigation, *Annu. Rev. Earth Planet. Sci.*, *33*, 195–214, doi:10.1146/annurev.earth.33.092203.122626.

Lancieri, M., and A. Zollo (2008), Bayesian approach to the real-time estimation of magnitude from the early *P* and *S* wave displacement peaks, *J. Geophys. Res.*, *113*, B12302, doi:10.1029/2007JB005386.

Li, H., A. Michelini, L. Zhu, F. Bernardi, and M. Spada (2007), Crustal velocity structure in Italy from analysis of regional seismic waveforms, *Bull. Seismol. Soc. Am.*, *97*(6), 2024–2039, doi:10.1785/0120070071.

Locati M., R. Camassi, and M. Stucchi (2011). DBMI11, la versione 2011 del Database Macrosismico Italiano. Milano, Bologna, doi:10.6092/INGV.IT-DBMI11. [Available at http://emidius.mi.ingv.it/DBMI11.]

Lomax, A., C. Satriano, and M. Vassallo (2012), Automatic picker developments and optimization: FilterPicker—A robust, broadband picker for real-time seismic monitoring and earthquake early warning, *Seismol. Res Lett*, *83*(3), 531–540, doi:10.1785/gssrl.83.3.531.

Luzi, L., S. Hailemikael, D. Bindi, F. Pacor, F. Mele, and F. Sabetta (2008), ITACA (ITalian ACcelerometric Archive): A web portal for the dissemination of Italian strong-motion data, *Seismol. Res. Lett.*, *79*(5), 716–722.

Meletti, C., F. Galadini, G. Valensise, M. Stucchi, R. Basili, S. Barba, G. Vannucci, and E. Boschi (2008), A seismic source zone model for the seismic hazard assessment of the Italian territory, *Tectonophysics*, *450*, 85–108.

Pacor, F., R. Paolucci, G. Ameri, M. Massa, and R. Puglia (2011), Italian strong motion records in ITACA: Overview and record processing, *Bull. Earthquake Eng.*, doi:10.1007/s10518-011-9295-x.

Picozzi, M., A. Emolo, C. Martino, A. Zollo, N. Miranda, G. Verderame, T. Boxberger, and REAKT Working Group (2015), Earthquake early warning system for schools: A feasibility study in southern Italy, *Seismol. Res. Lett.*, *86*(2), doi:10.1785/0220140194.

Pinsky, V. (2014), Modeling warning times for the Israel's earthquake early warning system, *J. Seismol.*, *19*(1), 121–139, doi:10.1007/s10950-014-9454-z.

Satriano, C., A. Lomax, and A. Zollo (2008), Real-time evolutionary earthquake location for seismic early warning, *Bull. Seismol. Soc. Am.*, *98*(3), 14821494, doi:10.1785/0120060159.

Satriano, C., Y.-M. Wu, A. Zollo, and H. Kanamori (2010), Earthquake early warning: Concepts, methods and physical grounds, *Soil Dyn. Earthquake Eng.*, *31*(2), 106–108, doi:10.1016/j.soildyn.2010.07.007.

Satriano, C., L. Elia, C. Martino, M. Lancieri, A. Zollo, and G. Iannaccone (2011), PRESTo, the earthquake early warning system for southern Italy: Concepts, capabilities and future perspectives, *Soil Dyn. Earthquake Eng.*, *31*(2), 137–153, doi:10.1016/j.soildyn.2010.06.008.

Zollo, A., O. Amoroso, M. Lancieri, Y. M. Wu, and H. Kanamori (2010), A threshold-based earthquake early warning using dense accelerometer networks, *Geophys. J. Int.*, *183*, 963–974, doi:10.1111/j.1365-246X.2010.04765.x.

Zollo A., S. Colombelli, L. Elia, A. Emolo, G. Festa, G. Iannaccone, C. Martino, and P. Gasparini (2014), An integrated regional and on-site earthquake early warning system for southern Italy: Concepts, methodologies and performances, in *Early Warning for Geological Disasters*, *Adv. Technol. Earth Sci.*, pp. 117–137, edited by F. Wenzel and J. Zschau, Springer, Berlin, doi:10.1007/978-3-642-12233-0_7.